Redox Biology 56 (2022) 102451

Contents lists available at ScienceDirect

Redox Biology

journal homepage: www.elsevier.com/locate/redox

TRIM7 modulates NCOA4-mediated ferritinophagy and ferroptosis in glioblastoma cells

Kaiqiang Li [a,b,d,1], Bingyu Chen [a,1], Aibo Xu [b,d,1], Jinglan Shen [a,b], Kaixuan Li [a,b,d], Ke Hao [a,b,d], Rongrong Hao [b,d], Wei Yang [a], Wanli Jiang [d,e], Yongfa Zheng [c,**], Feihang Ge [d,***], Zhen Wang [a,b,d,*]

[a] Center for Laboratory Medicine, Allergy Center, Department of Transfusion Medicine, Zhejiang Provincial People's Hospital (Affiliated People's Hospital, Hangzhou Medical College), Hangzhou, Zhejiang, 310014, China
[b] Key Laboratory of Biomarkers and In Vitro Diagnosis Translation of Zhejiang Province, Cancer Center, Zhejiang Provincial People's Hospital (Affiliated People's Hospital, Hangzhou Medical College), Hangzhou, Zhejiang, 310014, China
[c] Center of Oncology, Renmin Hospital of Wuhan University, Wuhan, 430060, China
[d] Hangzhou Chinese Academy of Sciences-Hangzhou Medical College Advanced Medical Technology Institute, Hangzhou, 310014, China
[e] Department of Thoracic Surgery, Renmin Hospital of Wuhan University, Wuhan, 430060, China

ARTICLE INFO

Keywords:
Glioblastoma
Ferroptosis
NCOA4
Ferritin
TRIM7

ABSTRACT

Objective: Glioblastoma is one of the most common intracranial malignant tumors with an unfavorable prognosis, and iron metabolism as well as ferroptosis are implicated in the pathogenesis of glioblastoma. The present study aims to decipher the role and mechanisms of tripartite motif-containing protein 7 (TRIM7) in ferroptosis and glioblastoma progression.

Methods: Stable TRIM7-deficient or overexpressing human glioblastoma cells were generated with lentiviral vectors, and cell survival, lipid peroxidation and iron metabolism were evaluated. Immunoprecipitation, protein degradation and ubiquitination assays were performed to demonstrate the regulation of TRIM7 on its candidate proteins.

Results: TRIM7 expression was elevated in human glioblastoma cells and tissues. TRIM7 silence suppressed growth and induced death, while TRIM7 overexpression facilitated growth and inhibited death of human glioblastoma cells. Meanwhile, TRIM7-silenced cells exhibited increased iron accumulation, lipid peroxidation and ferroptosis, which were significantly reduced by TRIM7 overexpression. Mechanistically, TRIM7 directly bound to and ubiquitinated nuclear receptor coactivator 4 (NCOA4) using K48-linked chains, thereby reducing NCOA4-mediated ferritinophagy and ferroptosis of human glioblastoma cells. Moreover, we found that TRIM7 deletion sensitized human glioblastoma cells to temozolomide therapy.

Conclusion: We for the first time demonstrate that TRIM7 modulates NCOA4-mediated ferritinophagy and ferroptosis in glioblastoma cells, and our findings provide a novel insight into the progression and treatment for human glioblastoma.

1. Introduction

Glioblastoma is one of the most common intracranial malignant tumors and remains incurable, with an unfavorable prognosis even following the standard treatments after diagnosis. Despite the development of surgical intervention, radiotherapy and temozolomide (TMZ) chemotherapy, the median survival rate of these patients is only approximately 1 year [1–5]. Ferroptosis is a novel form of programmed cell death and is mainly triggered by iron-induced accumulations of toxic lipid-based reactive oxygen species (ROS), which ultimately promotes polyunsaturated fatty acids peroxidation, membrane fragmentation and cell death [6–9]. Iron is essential for the execution of

* Corresponding author. Zhejiang Provincial People's Hospital (Affiliated People's Hospital, Hangzhou Medical College), Hangzhou, Zhejiang, 310014, China.
** Corresponding author.
*** Corresponding author.
E-mail addresses: zyf0322@126.com (Y. Zheng), fhge2018@163.com (F. Ge), wangzhen@hmc.edu.cn (Z. Wang).
[1] These authors contributed equally to this work.

https://doi.org/10.1016/j.redox.2022.102451
Received 8 August 2022; Accepted 19 August 2022
Available online 28 August 2022

ferroptosis, and regulation of intracellular iron homeostasis is often orchestrated by multiple molecular mechanisms regarding the uptake, export and release [10–12]. Ferritin is composed of ferritin heavy polypeptide 1 (FTH1) and ferritin light polypeptide 1, and functions as the major iron sequestration and storage protein to decrease intracellular iron concentrations. In contrast, ferritin proteolytic degradation leads to rapid releases of iron, and subsequently increases intracellular iron levels and ferroptosis [13–15]. Nuclear receptor coactivator 4 (NCOA4) is identified as a cargo receptor for the autophagic degradation of ferritin that is known as ferritinophagy, and NCOA4-mediated ferritin turnover contributes to the elevation of intracellular iron levels and subsequent ferroptosis in different cell types, including the glioblastoma cells [16,17]. In addition, transferrin (TF)/transferrin receptor (TFR)-mediated iron uptake and ferroportin 1 (FPN1)-mediated iron export are also implicated in maintaining intracellular iron concentrations [10,12,18]. Intriguingly, glioblastoma cells are especially sensitive to intracellular iron levels due to the alterations of various iron-dependent enzyme activities and iron metabolism-related proteins [19]. Accordingly, emerging studies have demonstrated indispensable roles of iron metabolism and ferroptosis in glioblastoma progression. Zhu et al. reported that ferroptosis signature was different in human glioblastoma, and that some hub ferroptosis-related genes could independently predict the prognosis of glioblastoma patients [20]. And findings from Buccarelli et al. and Chen et al. revealed that igniting ferroptosis significantly enhanced susceptibility of glioblastoma cells and glioblastoma stem cells to TMZ treatment, thereby reducing recurrence and extending the survival period of glioblastoma patients [21,22]. Based on these results, it is reasonable to treat human glioblastoma through targeting ferroptosis.

Tripartite motif-containing proteins (TRIMs) are a family of E3 ubiquitin ligases and mediate endogenous proteins for degradation by the ubiquitin-proteasome system [23,24]. TRIMs are implicated in the pathogenesis of various human tumors, including the glioblastoma. Liu et al. identified TRIM3 as a tumor suppressor, and TRIM3 downregulation accelerated the growth and proliferation of glioblastoma cells [25]. Feng et al. demonstrated that TRIM14 overexpression evidently promoted epithelial-mesenchymal transition in glioblastoma cells, and that its level correlated with glioblastoma progression and shorter patient survival times [26]. A very recent study by Ji et al. indicated that TRIM22 activated nuclear factor-κB pathway through its E3 ligase activity, and subsequently promoted glioblastoma cell proliferation *in vivo* and *in vitro* [27]. TRIM7 is a member of TRIMs family and contains an N-terminal RING finger, a B-box domain, a coiled-coil domain and a C-terminal PRY/SPRY domain [28]. TRIM7 is dysregulated in various human tumors, and positively or negatively regulates tumor cell proliferation. Chakraborty et al. reported that TRIM7 mediated K63-linked ubiquitination and subsequent protein stabilization of RING domain AP-1 co-activator 1, thereby increasing cell growth and lung tumor burden [29]. Meanwhile, Zhou et al. found that TRIM7 promoted osteosarcoma cell migration and invasion through ubiquitinating breast cancer metastasis suppressor 1 at the K184 site [30]. In contrast, other findings showed that TRIM7 could suppressed tumor growth *in vivo* and *in vitro* [31–33]. In the present study, we aim to decipher the role and mechanisms of TRIM7 in the progression of glioblastoma.

2. Materials and methods

2.1. Chemicals

Ferrostain-1 (Fer-1, #S7243), liproxstatin-1 (Lip-1, #S7699), deferoxamine mesylate (DFO, #S5742), ciclopirox ethanolamine (CPX, #S3019), erastin (#S7242), RSL3 (#S8155), 3-methyladenine (3-MA, #S2767) and chloroquine (CQ, #S6999) were purchased from Selleck Chemicals (Houston, TX, USA). Necrosulfonamide (NSA, #ab143839; a necroptosis inhibitor), Z-VAD (OH)-FMK (Z-VAD, #ab120382; an irreversible general caspase inhibitor), BrdU Cell Proliferation ELISA Kit (#ab126556), lactate dehydrogenase (LDH) assay kit (#ab65393) and colorimetric Iron Assay Kit (#ab83366) were obtained from Abcam (Cambridge, UK). Ferric ammonium citrate (FAC, #RES20400-A7), cycloheximide (CHX, #01810), MG132 (proteasome inhibitor, #M7449), temozolomide (TMZ, #T2577), cell counting kit-8 (CCK-8, #96992) and Lipid Peroxidation Assay Kit (#MAK085) were purchased from Sigma-Aldrich (St. Louis, MO, USA). Lipofectamine™ 3000 Transfection Reagent (#L3000001), Pierce BCA Protein Assay Kit (#23225), Amplex Red Hydrogen Peroxide/Peroxidase Assay Kit (#A22188) and B27 (#17504044) were purchased from ThermoFisher Scientific (Rockford, IL, USA). Basic fibroblast growth factor (bFGF, #AF-100-18B) and epidermal growth factor (EGF, #AF-100-15) were purchased from Peprotech (Cranbury, NJ, USA). Lipid Peroxidation Assay Kit (#A106) was purchased from Nanjing Jiancheng Bioengineering Institute (Jiangsu, China). Dihydroethidium (DHE, #S0063) was purchased from Beyotime (Shanghai, China). Human TRIM7 isoform 1 cDNA (#RG224754) was cloned from Origene Technologies (Rockville, MD, USA) and then transferred into the lentiviral expression vector by GeneChem Co., Ltd. (Shanghai, China). Three short hairpin RNA sequences against human TRIM7 (sh*TRIM7*) or sh*NCOA4* carried by lentivirus were generated by GeneChem Co., Ltd., and the oligonucleotide sequences (sense strand) were provided in Online Supplementary Table I.

2.2. Cell lines and treatments

Two human normal brain astroglia cells (SVG and HA1800), two human glioblastoma cells (A172 and U87MG) and HEK293T cells were purchased from ATCC (Manassas, VA, USA), and cultured in DMEM medium containing 10% fetal bovine serum. To construct stable TRIM7-deficient glioblastoma cells, A172 and U87MG cells were infected with sh*TRIM7* at a multiplicity of infection (MOI) of 10. After 48 h of infection, the cells were incubated with puromycin (2 μg/mL) for 14 days to select the stable expression cells, and the stable TRIM7-knockdown clones were validated by immunoblot (IB), whereas the cells stably transfected with scramble control sh*RNA* vector were used as the negative control [17,31]. Meanwhile, stable TRIM7-overexpressing glioblastoma cells were also constructed using the lentiviral system. In addition, *CRISPR/Cas9* system was applied to generate TRIM7-knockout (KO) glioblastoma cells as previously described [31]. Briefly, A172 cells were transfected with a sgRNA targeting TRIM7 (Online Supplementary Table I) using the pLentiCRISPRv2 system, followed by a puromycin (2 μg/mL) selection. The non-specific sgRNA-transfected cells were used as the wild type (WT) control. The surviving colonies were passaged and validated by IB. To inhibit ferroptosis, necroptosis or apoptosis, TRIM7-deficient cells were incubated with Fer-1 (1 μmol/L), Lip-1 (0.2 μmol/L), NSA (0.5 μmol/L) or Z-VAD (10 μmol/L) as previously described [12,34]. To chelate intracellular iron, sh*TRIM7*-infected glioblastoma cells were incubated with DFO (100 μmol/L, membrane impermeable) or CPX (5 μmol/L, membrane permeable) [12,17]. In contrast, FAC was used to increase intracellular iron levels of TRIM7-deficient cells as previously described [17]. To induce ferroptosis of glioblastoma cells, TRIM7-overexpressing A172 and U87MG cells were stimulated with erastin (5 μmol/L) or RSL3 (2 μmol/L) for 72 h [12]. To inhibit autophagy, TRIM7-deficient A712 cells were incubated with 3-MA (10 mmol/L) or CQ (3 μmol/L) [17]. To silence endogenous NCOA4, TRIM7-deficient A712 cells were infected with the lentiviral vectors carrying sh*NCOA4* at a MOI of 10 for 12 h, and then maintained in fresh DMEM medium for an additional 72 h. Moreover, WT or KO A172 cells were incubated with TMZ (100 μmol/L) to further determine whether TRIM7 KO could sensitize glioblastoma cells to TMZ chemotherapy [22].

To investigate the necessity of RING domain in TRIM7-mediated NCOA4 degradation, Cys29 and Cys32 in the RING finger were mutated to Ala (Flag-TRIM7 CA) to destroy the integrity of the RING domain [29]. Meanwhile, we mutated a conserved Try57 to Ala

(Flag-TRIM7 WA) to block the interaction of the RING domain with ubiquitin-conjugating enzymes [29]. The WT and these mutant plasmids of human TRIM7 were co-transfected with HA-NCOA4 into HEK293T cells for 72 h using a Lipofectamine™ 3000 Transfection Reagent. In addition, DNA fragments encoding various truncated TRIM7 were also generated, which were then co-transfected with HA-NCOA4 plasmid into HEK293T cells for 72 h to determine specific domains for the interaction between TRIM7 and NCOA4.

2.3. Protein degradation assay

To investigate whether TRIM7 destabilized NCOA4 protein, TRIM7-overexpressing or control A172 cells were incubated with CHX (10 μmol/L) to inhibit protein synthesis, and cell lysates were prepared at 0, 3, 6 and 9 h for IB analysis [35]. In addition, TRIM7-overexpressing A172 cells were treated with MG132 (10 μmol/L) for 6 h to suppress proteasome-mediated protein degradation [28,31].

2.4. Cell growth and proliferation

Cell growth was measured by CCK-8 method as previously described [36,37]. Briefly, cells were incubated with 10% CCK-8 solution at 37 °C for 4 h, and then the absorbance was detected at 450 nm. Cell proliferation was determined by a BrdU Cell Proliferation ELISA Kit according to a previous study [38]. In addition, colony formation assay was also performed to evaluate glioblastoma cells proliferation [39,40]. Briefly, glioblastoma cells were seeded into 6-well plates and cultured for 14 days, which were then fixed in methanol for 30 min, stained with 0.5% crystal violet at room temperature for 15 min and carefully rinsed with tap water. The colonies larger than 50 μm were scored in a blinded manner.

2.5. Cell death analysis

Cell death was analyzed by measuring LDH releases in the medium using a commercial kit [17,41,42]. Briefly, cells were removed by a 600×*g* centrifugation, and cell-free medium solution was incubated with WST Substrate Mix and LDH Reaction Mix at room temperature for 30 min. The absorbance was measured at 450 nm and used to calculate cell death ratio as previously described.

2.6. IB and immunoprecipitation (IP)

Cell lysates were prepared using RIPA lysis buffer and total protein concentrations were assessed by a Pierce BCA Protein Assay Kit. Next, 20 μg proteins were separated by 10% SDS-PAGE and transferred onto PVDF membranes. Membranes were blocked by 5% skimmed milk at room temperature for 2 h and incubated with the primary antibodies at 4 °C overnight. The primary antibodies were listed as the Online Supplementary Table II. On the second day, membranes were incubated with horse radish peroxidase (HRP)-conjugated secondary antibodies at room temperature for 2 h, and the blots were visualized by electrochemiluminescence substrate. Protein expression was normalized to endogenous GAPDH using the Image Lab software (Version 6.0) [43–45]. HEK293T cells expressing HA-NCOA4 and various truncated TRIM7 were lysed and subjected to Flag IP, and then proteins were washed from the beads, boiled and separated by SDS-PAGE [46,47].

2.7. Quantitative real-time PCR

Total RNA was extracted using TRIzol reagent and reversely transcribed to cDNA using a Maxima First Strand cDNA Synthesis Kit (Roche) according to the manufacturer's instructions as previously described [48,49]. Quantitative real-time PCR was performed with SYBR Green incorporation. The primer sequences were listed as below: human TRIM7, forward: 5′-GCTCGGGGTTGAGATCACC-3′, reverse: 5′-CCAGGCACATT GCTACACCT-3'; human NCOA4, forward: 5′-CAGCAGCTCTACTCGT TATTGG-3′, reverse: 5′-TCTCCAGGCACACAGAGACT-3'; human GAPDH, forward: 5′-GCACCGTCAAGGCTGAGAAC-3′, reverse: 5′-TGGTGAA-GACGCCAGTGGA-3'. Gene expression was calculated with the $2^{-\triangle\triangle Ct}$ method and normalized to the internal control GAPDH.

2.8. Iron assay

Intracellular ferrous iron levels were analyzed using a colorimetric Iron Assay Kit according to the manufacturer's instructions. Briefly, cells were lysed in Iron Assay Buffer on ice and centrifuged at 16000×*g* for 10 min to remove insoluble materials. And then the supernatants were collected, incubated with assay buffer at 37 °C for 30 min, followed by an incubation with 100 μL Iron Probe for an additional 1 h. Finally, the absorbance was immediately measured at 593 nm, and iron concentrations were calculated by the standard calibration curve method. Labile iron pool (LIP) was detected by using calcein acetoxymethyl ester as previously described [12]. Briefly, cells were incubated with calcein (2 μmol/L) at 37 °C for 30 min, and then mixed with DFO (100 μmol/L) to remove calcein from iron. The change in fluorescence at 485 nm excitation and 535 nm emission before- and post-DFO addition was calculated as the level of LIP.

2.9. Lipid peroxidation measurements

Lipid peroxidation was assessed by measuring intracellular lipid peroxidase (LPO) level using a commercial kit following the manufacturer's instructions. Briefly, cells were lysed, and incubated with Reagents 1 and Reagents 2 at 45 °C for 1 h. Next, the samples were centrifuged at 4000×*g* for 10 min, and cell-free supernatants were collected to detect LPO level at 586 nm. The level of intracellular malondialdehyde (MDA) was detected by a Lipid Peroxidation Assay Kit to further evaluate lipid peroxidation as previously described [50,51]. Briefly, cells were lysed on ice in the MDA Lysis Buffer and centrifuged at 13000×*g* for 10 min to remove insoluble materials. Next, the supernatants were incubated with TBA solution at 95 °C for 1 h, cooled down to room temperature and measured at 532 nm. In addition, we also detected the productions of hydrogen peroxide (H_2O_2) and superoxide anion to evaluate oxidative stress as previously described. Briefly, cell samples were prepared and incubated with Amplex Red reagent (100 μmol/L) and HRP (0.2 U/mL) at room temperature for 30 min protected from light, and then the absorbance was measured at 560 nm [35]. Superoxide anion levels were detected by incubating glioblastoma cells with DHE probe (10 mmol/L) at 37 °C for 30 min, and the fluorescence was measured at 485 nm excitation and 530 nm emission [17].

2.10. In vivo and in vitro ubiquitination assays

For *in vivo* ubiquitination assays, HA-NCOA4 and His-ubiquitin (His-Ub) plasmids were transfected into HEK293T cells with or without Flag-TRIM7 using a Lipofectamine™ 3000 Transfection Reagent. After 72 h, cells were lysed and subjected to IP assay with anti-HA antibody-conjugated agarose beads. After washing for 5 times, proteins were eluted from the beads and subjected to IB analysis. To identify the chain linkage of ubiquitinated NCOA4, HEK293T cells were transfected with two ubiquitin mutants, K48R and K63R, as previously described [29]. For *in vitro* ubiquitination assays, the tested proteins were expressed by a TNT Quick Coupled Transcription/Translation System (Promega, Madison, WI, USA) according to the manufacturer's instructions. The Flag-TRIM7 and HA-NCOA4 proteins were mixed with ubiquitin conjugation mixture (Enzo Life Sciences, Farmingdale, NY, USA) at 30 °C for 1 h, and the samples were subjected to IP assay as aforementioned.

2.11. Clinical specimens and cell isolation

The collection and use of clinical specimens were approved by the

Ethics Committee of Zhejiang Provincial People's Hospital, and also were in accordance with the instructions from Declaration of Helsinki. All patients or the families have signed the informed written consent. Normal brain tissues were collected from patients with traumatic brain injury during emergency surgeries. Human glioblastoma cells were immediately isolated from 2 patients after dissociation of primary tumor or after transient xenograft passage. To stimulate the recovery of GSCs, human glioblastoma cells were cultivated in Neurobasal-A medium with B27, bFGF (20 ng/mL) and EGF (20 ng/mL) as previously described [52,53]. The knockdown of TRIM7 or NCOA4 was achieved through lentiviral vectors as mentioned above. For TMZ treatment, cells were incubated with TMZ (500 μmol/L) for indicating times [54].

2.12. Subcutaneous and intracranial tumor xenograft models

To investigate whether TRIM7-KO A172 cells were more sensitive to TMZ treatment *in vivo*, 1×10^6 TRIM7-KO or WT A172 cells were subcutaneously injected into the flanks of non-obese diabetic-severe combined immunodeficient NOD-SCID mice at 4–6 weeks of age [52,55]. Ten days after inoculation, mice were intraperitoneally injected with TMZ (5 mg/kg) three times every week [22,54]. To imitate the clinical process of human glioblastoma and enhance the translational value of our findings, we also established patient-derived xenograft (PDX) models *in vivo* as previously described [55]. Briefly, 1×10^6 human glioblastoma cells from primary tumors or transient xenografts with or without TRIM7 silence were subcutaneously injected into the flanks of NOD-SCID mice in the presence or absence of TMZ treatment. Tumors were observed daily with tumor volume calculated weekly using the following formula: (length × width^2)/2. At the end of study, tumors were carefully excised and weighed to obtain the tumor weight. In addition, mice were also intracranially injected at 3 mm lateral and 3 mm depth of the bregma with TRIM7-silenced or control human glioblastoma cells expressing luciferase reporter as previously described. Tumor growth was monitored by an In Vivo Imaging System Spectrum imaging system (PerkinElmer, Waltham, MA, USA) at indicated times.

2.13. Statistical analysis

All values are presented as the mean ± S.D., and analyzed by GraphPad Prism software (Version 7.0). Data from 3 or more groups with normal distributions were compared using one-way ANOVA followed by Tukey post-hoc analysis, while comparisons between 2 groups were performed using an unpaired two-tailed Student's *t*-test. $P < 0.05$ is considered statistically significant.

3. Results

3.1. TRIM7 expression is elevated in human glioblastoma cells and tissues

To investigate the role of TRIM7 in glioblastoma progression, we first detected its expression in human glioblastoma cells. As shown in Fig. 1A, compared to human normal brain astroglia cells (SVG and HA1800), human glioblastoma cells (A172 and U87MG) exhibited higher TRIM7 protein levels. And our findings also revealed that TRIM7 expression was elevated in human glioblastoma tissues (Fig. 1B). Collectively, these results suggest that TRIM7 may be implicated in the progression of glioblastoma.

3.2. TRIM7 silence suppresses growth and induces death of human glioblastoma cells

We next evaluated the biological effects of TRIM7 by generating stable TRIM7-deficient glioblastoma cells. As shown in Fig. 2A, A172 or U87MG cells transfected with two independent sh*TRIM7*, named sh*TRIM7*-2 and sh*TRIM7*-3, were used in our further study due to their knockdown efficiency. Intriguingly, we found that TRIM7 knockdown significantly suppressed glioblastoma cell growth (Fig. 2B). In colony formation and BrdU cell proliferation assays, cell proliferation was also reduced in A172 or U87MG cells with TRIM7 silence (Fig. 2C–D). To investigate the mechanisms mediating cell growth inhibition in the context of TRIM7 silence, we assessed cell death by detecting LDH releases to the medium. As shown in Fig. 2E, the releases of LDH significantly increased in glioblastoma cells with loss of TRIM7. To further validate whether TRIM7 silence could induce cell death of human

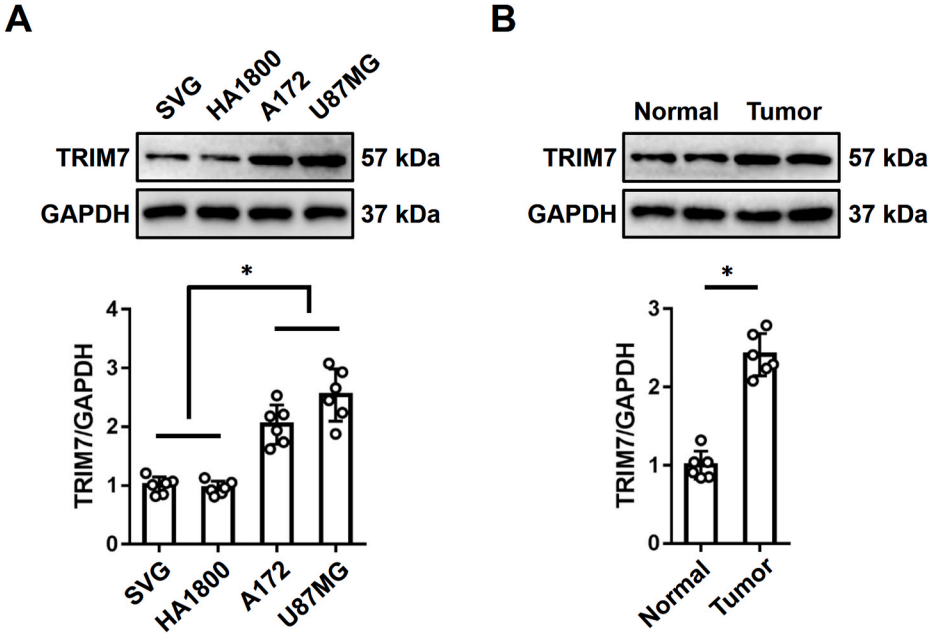

Fig. 1. TRIM7 expression is elevated in human glioblastoma cells and tissues. (A) Human normal brain astroglia cells (SVG and HA1800) and human glioblastoma cells (A172 and U87MG) were subjected to IB assay to detect TRIM7 expression. (B) The expression of TRIM7 protein in human glioblastoma tissues. $N = 6$ for each group. All values are presented as the mean ± S.D., $^*P < 0.05$ is considered statistically significant.

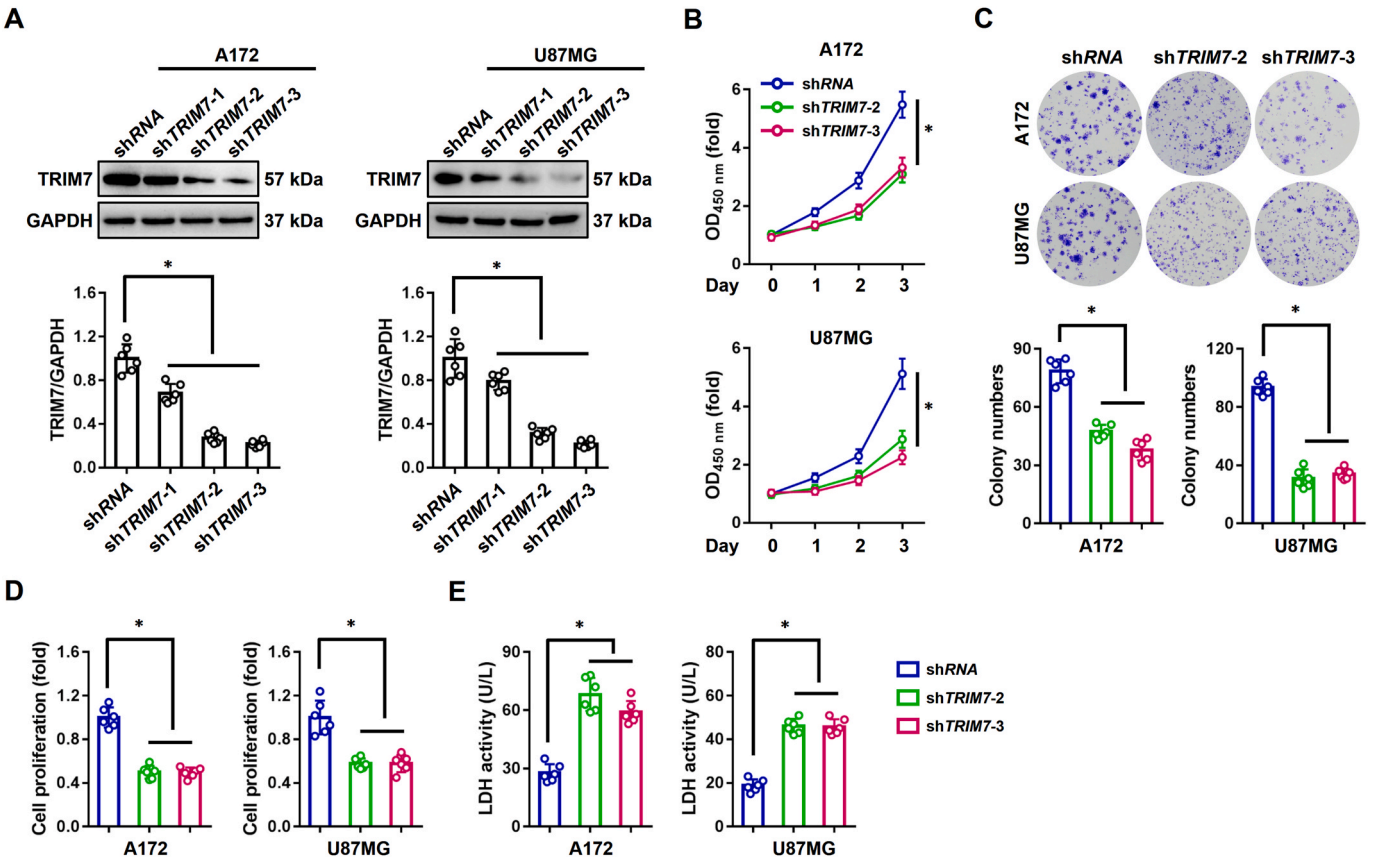

Fig. 2. TRIM7 silence suppresses growth and induces death of human glioblastoma cells. (A) Stable TRIM7-deficient cells were subjected to IB assay to validate the efficiency. (B) Stable TRIM7-deficient or control cells were cultured and exposed to CCK-8 assay to evaluate cell viability. (C) Colony formation assay. (D) Cell proliferation was assessed by BrdU assay at 72 h. (E) LDH releases from human glioblastoma cells to the medium at 72 h. $N = 6$ for each group. All values are presented as the mean ± S.D., $^*P < 0.05$ is considered statistically significant.

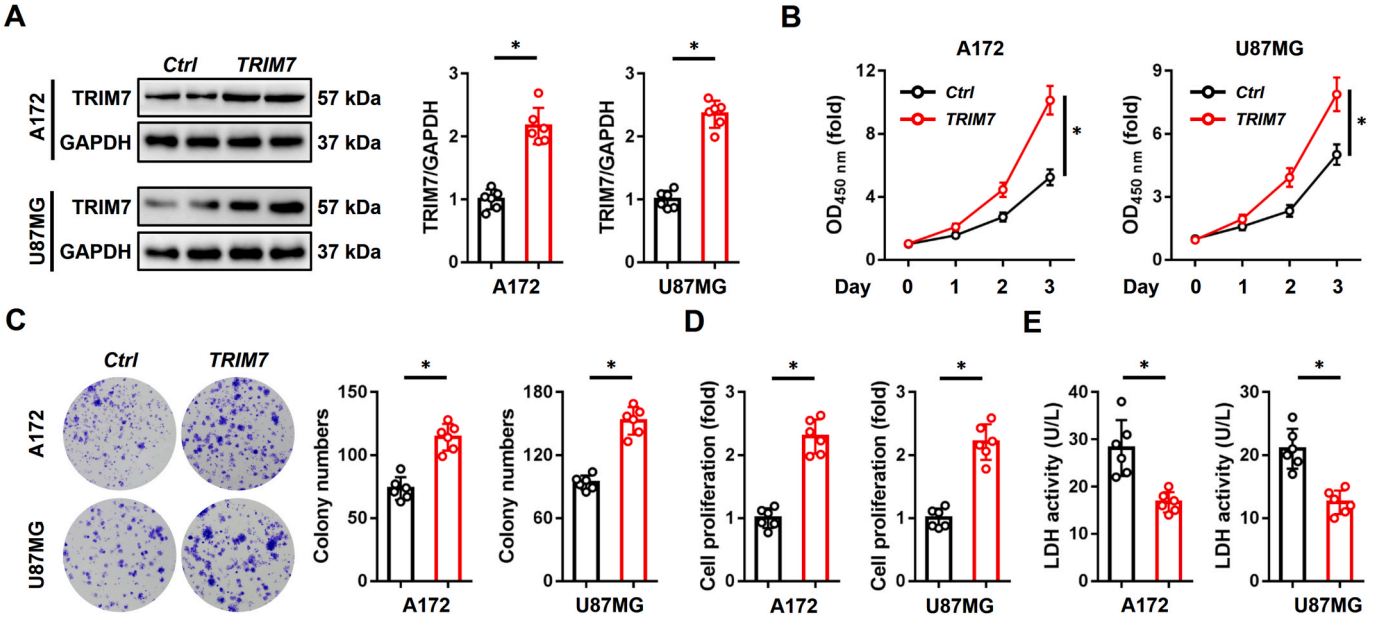

Fig. 3. TRIM7 overexpression accelerates growth and inhibits death of human glioblastoma cells. (A) Stable TRIM7-overexpressing cells were subjected to IB assay to validate the efficiency. (B) Stable TRIM7-overexpressing or control cells were cultured and exposed to CCK-8 assay to evaluate cell viability. (C) Colony formation assay. (D) Cell proliferation was assessed by BrdU assay at 72 h. (E) LDH releases from human glioblastoma cells to the medium at 72 h. $N = 6$ for each group. All values are presented as the mean ± S.D., $^*P < 0.05$ is considered statistically significant.

glioblastoma cells, we generated a TRIM7-KO A172 cells using the *CRISPR/Cas9* system (Fig. S1A). As shown in Figs. S1B–E, TRIM7-deficient A172 cells exhibited lower cell viability and proliferative capacity. In addition, more cell death was observed in human glioblastoma cells after ablating TRIM7, as evidenced by the increased LDH releases (Fig. S1F). These findings indicate that TRIM7 silence suppresses growth and induces death of human glioblastoma cells.

3.3. TRIM7 overexpression accelerates growth and inhibits death of human glioblastoma cells

Next, we overexpressed TRIM7 in A712 and U87MG cells, and the efficiency was validated by IB assay (Fig. 3A). As shown in Fig. 3B, the viability of TRIM7-overexpressing glioblastoma cells was dramatically increased. Colony formation and BrdU cell proliferative assays further revealed that TRIM7 overexpression facilitated survival of human glioblastoma cells (Fig. 3C–D). In contrast, cell death was inhibited by TRIM7 overexpression, as evidenced by the decreased LDH releases (Fig. 3E). In aggregate, we demonstrate that TRIM7 overexpression accelerates growth and inhibits death of human glioblastoma cells.

3.4. TRIM7 silence causes intracellular iron accumulation and ferroptosis of human glioblastoma cells

We further explored the possible type of cell death that contributed to TRIM7 silence-mediated glioblastoma suppression by using pharmacological inhibitors of different forms of cell death. As shown in Fig. 4A, two independent ferroptosis inhibitors (Fer-1 and Lip-1) significantly blocked the loss of glioblastoma cells after knocking down TRIM7, which was only slightly affected by necroptosis inhibitor (NSA) or apoptosis inhibitor (Z-VAD). These results implied that the decreased viability in TRIM7-silenced glioblastoma cells was mainly attributable to the induction of ferroptosis, rather than necroptosis or apoptosis. In addition, both Fer-1 and Lip-1 treatment significantly reduced LDH releases from TRIM7-silenced cells (Fig. 4B). To further evaluate the involvement of ferroptosis in TRIM7 knockdown-mediated glioblastoma suppression, we measured some ferroptotic markers. Lipid peroxidation is a key feature of ferroptosis, and the final product of lipid peroxidation is MDA. As shown in Fig. 4C–D, the levels of LPO and MDA were significantly increased in TRIM7-silenced glioblastoma cells. Intracellular ROS, including H_2O_2 and superoxide anion, is the main factor to induce lipid peroxidation and ferroptosis. As expected, TRIM7 knockdown significantly elevated intracellular H_2O_2 and superoxide anion

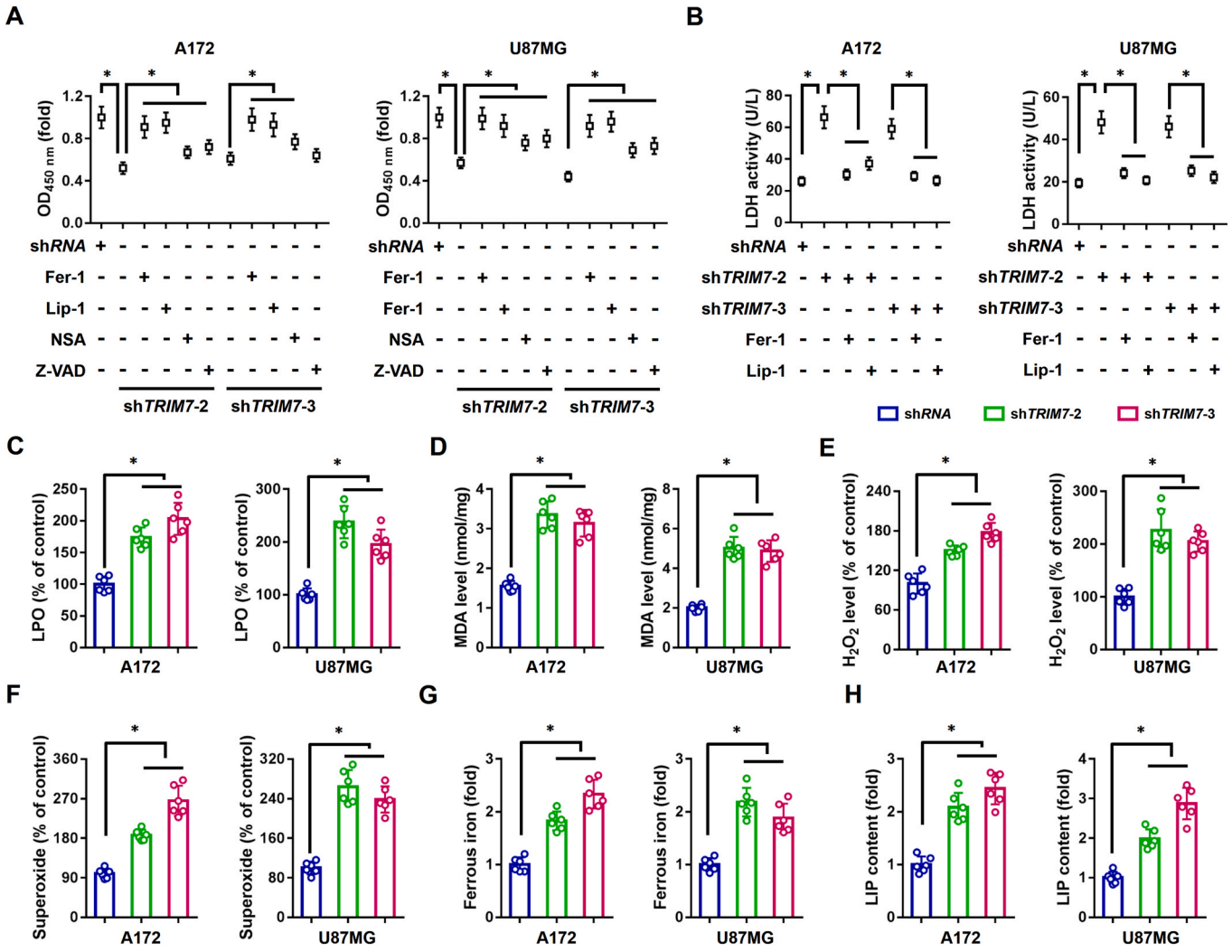

Fig. 4. TRIM7 silence causes intracellular iron accumulation and ferroptosis of human glioblastoma cells. (A) Stable TRIM7-deficient cells were treated with inhibitors of ferroptosis (Fer-1 and Lip-1), necroptosis (NSA) and apoptosis (Z-VAD), and then cell viability was measured using CCK-8 assay at 72 h. (B) LDH releases from human glioblastoma cells to the medium at 72 h. (C) Relative LPO level. (D) Quantification of MDA content. (E–F) The levels of H_2O_2 and superoxide anion in human glioblastoma cells. (G–H) Intracellular ferrous iron and LIP levels. $N = 6$ for each group. All values are presented as the mean ± S.D., $^*P < 0.05$ is considered statistically significant.

levels in A172 and U87MG cells (Fig. 4E–F). Iron contributes to the execution of ferroptosis and can facilitate ROS generation through the Fenton reaction. Therefore, we evaluated whether TRIM7 silence altered intracellular iron levels. As shown in Fig. 4G, the levels of ferrous iron, an active form of intracellular iron in mediating lipid peroxidation and ferroptosis, were significantly elevated in human glioblastoma cells with TRIM7 silence. LIP is a pool of redox-active iron and functions as the direct source of the Fenton reaction. Our results suggested that TRIM7 silence also increased intracellular LIP levels in human glioblastoma cells (Fig. 4H). Meanwhile, increased levels of lipid peroxidation and intracellular iron were also detected in TRIM7-KO A172 cells (Figs. S2A–D). To test whether increased iron levels were the cause of cell loss in TRIM7-silenced cells, these cells were exposed to different iron chelators. As shown in Figs. S3A–B, the decreased viability and increased LDH releases in TRIM7-silenced cells were significantly blocked by either DFO or CPX. In contrast, increasing intracellular iron through exposure to FAC led to further increases of death in sh*TRIM7*-transfected cells (Figs. S3C–D). Taken together, our results reveal that TRIM7 silence causes intracellular iron accumulation and ferroptosis of human glioblastoma cells.

3.5. *TRIM7 overexpression reduces ferroptosis of human glioblastoma cells*

We also investigated whether TRIM7 overexpression could alleviate erastin- or RSL3-induced ferroptosis of human glioblastoma cells. Consistent with previous studies, both erastin and RSL3 treatment elevated LPO and MDA levels, indicating an increase of lipid peroxidation, which, however, were significantly suppressed by TRIM7 overexpression (Fig. 5A–B). As expected, both erastin- and RSL3-induced cell losses were prevented in TRIM7-overexpressed human glioblastoma cells (Fig. 5C–D). From these results, we conclude that TRIM7 overexpression reduces ferroptosis of human glioblastoma cells.

3.6. *TRIM7 silence promotes NCOA4-mediated ferritinophagy and ferroptosis of human glioblastoma cells*

To determine the mechanisms underlying intracellular iron accumulation by TRIM7, IB analysis was performed to detect levels of iron regulatory proteins. Intracellular iron homeostasis is primarily regulated by TF/TFR-mediated iron uptake and FPN1-mediated iron export; however, we found that neither TF/TFR nor FPN1 expression was affected by TRIM7 silence (Fig. 6A). Iron regulatory protein 2 (IRP2) registers cytosolic iron levels and post-transcriptionally controls iron metabolism genes expression to optimize cellular iron availability by binding to iron-responsive elements. Yet, IB results showed no significant alteration of IRP2 protein levels in TRIM7-silenced human glioblastoma cells (Fig. 6A). Ferritin is required for intracellular iron storage and its proteolytic degradation results in rapid releases of free iron [16]. Interestingly, significant decreases of FTH1 were observed in TRIM7-silenced A172 cells (Fig. 6A–B). And TRIM7-KO A172 cells also exhibited lower FTH1 protein expression (Fig. 6C). NCOA4 is a cargo

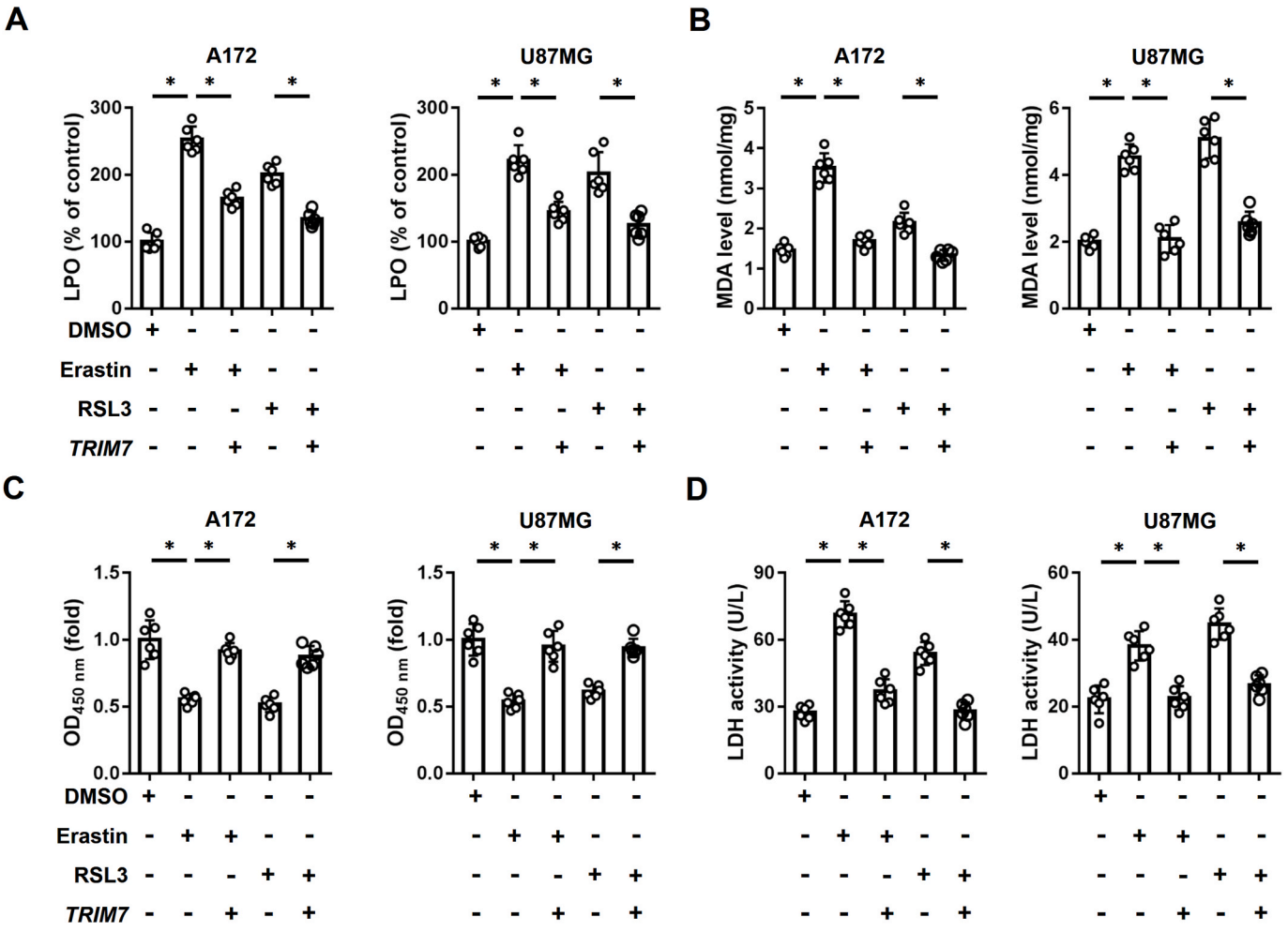

Fig. 5. TRIM7 overexpression reduces ferroptosis of human glioblastoma cells. (A) TRIM7-overexpressing or control cells were stimulated with erastin or RSL3 for 72 h, and relative LPO level was determined. (B) Quantification of MDA content. (C) Cell viability was measured using CCK-8 assay. (D) LDH releases from human glioblastoma cells to the medium. $N = 6$ for each group. All values are presented as the mean ± S.D., $^*P < 0.05$ is considered statistically significant.

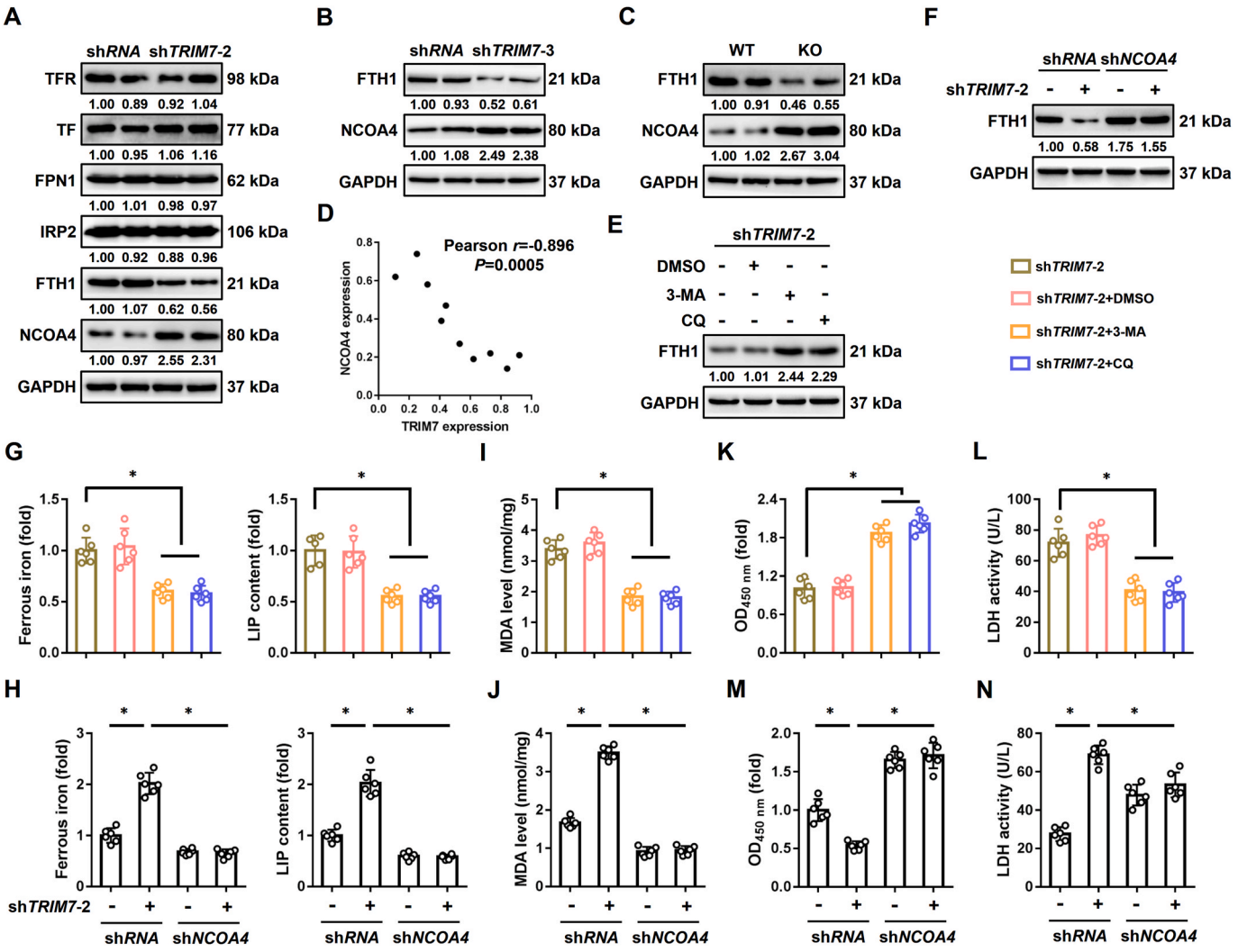

Fig. 6. TRIM7 silence promotes NCOA4-mediated ferritinophagy and ferroptosis of human glioblastoma cells. (A–C) Relative protein levels of TFR, TF, FPN1, IRP2, FTH1 and NCOA4 in human glioblastoma cells with or without TRIM7 deficiency. (D) *TRIM7* and *NCOA4* mRNA levels in human glioblastoma cells. (E) Stable TRIM7-deficient cells were treated with 3-MA or CQ to inhibit autophagy, and then subjected to IB assay to detect FTH1 protein. (F) Stable TRIM7-deficient cells were infected with or without sh*NCOA4*, and then subjected to IB assay to detect FTH1 protein. (G–H) Ferrous iron and LIP levels in stable TRIM7-deficient cells with autophagic inhibition or NCOA4 silence. (I–J) Quantification of MDA content. (K–N) Cell viability and LDH releases. $N = 6$–10 for each group. All values are presented as the mean ± S.D., $^*P < 0.05$ is considered statistically significant.

receptor for the autophagic degradation of ferritin, and NCOA4-mediated ferritinophagy contributes to ferritin degradation, elevation of intracellular iron levels and subsequent ferroptotic cell death [16]. As shown in Fig. 6A–C, NCOA4 protein levels were significantly elevated by TRIM7 silence in A172 cells. In addition, we found a negative correlation between *TRIM7* and *NCOA4* mRNA levels in human glioblastoma tissues (Fig. 6D). To investigate the role of autophagy in mediating ferritin degradation, TRIM7-silenced A172 cells were treated with 3-MA or CQ to suppress autophagosome assembly or the fusion of autophagosomes and lysosomes. As shown in Fig. 6E, FTH1 protein levels were increased when cells were treated with 3-MA or CQ. Moreover, NCOA4 knockdown also dramatically blunted FTH1 degradation in TRIM7-silenced A172 cells (Fig. 6F). As expected, the increased level of intracellular ferrous iron and LIP in sh*TRIM7*-infected cells were significantly reduced by autophagic inhibition or NCOA4 knockdown, followed by an inhibition of lipid peroxidation (Fig. 6G–J). Consistently, both autophagic inhibition and NCOA4 silence significantly reduced death and facilitated survival of A172 cells with TRIM7 knockdown (Fig. 6K-N). To imitate the clinical process of human glioblastoma and enhance the translational value of our findings, we also evaluated the role of TRIM7 in human GSCs and PDX models *in vitro* and *in vivo*. As shown in Figs. S4A–C, TRIM7 silence inhibited survival and induced death of human GSCs. And we also found that TRIM7 knockdown facilitated ferroptotic cell death of GSCs, as evidenced by the increased levels of MDA, ferrous iron and LIP (Figs. S4D–F). In addition, significant decreases of FTH1 protein were observed in TRIM7-silenced GSCs, which were prevented by NCOA4 knockdown (Fig. S4G). NCOA4 silence also reduced accumulations of intracellular ferrous iron and LIP, and significantly blocked lipid peroxidation in TRIM7-silenced GSCs (Figs. S4H–J). Accordingly, TRIM7 silence-induced elevation of LDH releases was also attenuated by NCOA4 knockdown (Fig. S4K). In line with the *in vitro* findings, we demonstrated that TRIM7 silence significantly suppressed the growth of human glioblastoma in subcutaneous and intracranial PDX models, as evidenced by the decreased tumor volume and weight (Fig. S4L-O). These results demonstrate that TRIM7 silence promotes NCOA4-mediated ferritinophagy and ferroptosis of human glioblastoma cells.

3.7. TRIM7 directly binds to and ubiquitinates NCOA4 using K48-linked chains

We also measured how TRIM7 regulated NCOA4 level. Our data

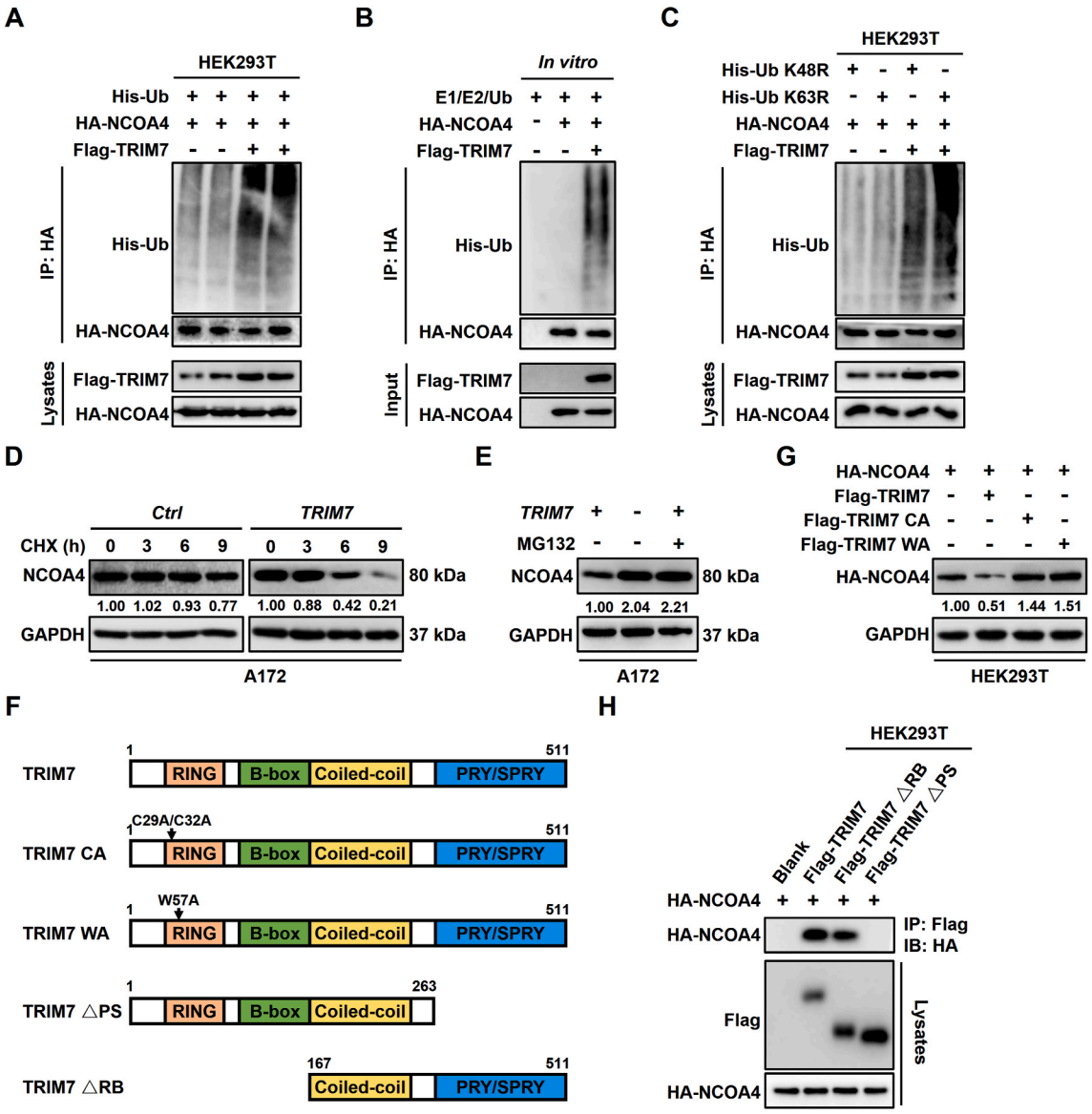

Fig. 7. TRIM7 directly binds to and ubiquitinates NCOA4 using K48-linked chains. (A) His-Ub and HA-NCOA4 plasmids were co-transfected into HEK293T cells with or without Flag-TRIM7 plasmid, and then cell lysates were prepared to IP assay with anti-HA antibody-conjugated agarose beads. (B) The Flag-TRIM7 and HA-NCOA4 proteins were mixed with ubiquitin conjugation mixture at 30 °C for 1 h, and then subjected to IP assay with anti-HA antibody-conjugated agarose beads. (C) HA-NCOA4 plasmid-transfected HEK293T cells with or without TRIM7 overexpression were transfected with different ubiquitin mutant plasmids, and then cell lysates were prepared to IP assay with anti-HA antibody-conjugated agarose beads. (D) Stable TRIM7-overexpressing A172 cells were treated with CHX to inhibit protein synthesis, and then NCOA4 protein levels were determined by IB assay. (E) Stable TRIM7-overexpressing A172 cells were treated with or without MG132, and then NCOA4 protein levels were determined. (F–G) HA-NCOA4 plasmid was co-transfected into HEK293T cells with different mutant TRIM7 plasmids, and then cell lysates were prepared to IB assay. (H) HA-NCOA4 plasmid was co-transfected into HEK293T cells with different truncated TRIM7 plasmids, and then cell lysates were prepared to IP assay with anti-Flag antibody-conjugated agarose beads. $N = 6$ for each group. All values are presented as the mean ± S.D., $^*P < 0.05$ is considered statistically significant.

showed that neither deficiency nor overexpression of TRIM7 affected NCOA4 mRNA levels in human glioblastoma cells (Figs. S5A–C). TRIM7 functions as an E3 ubiquitin ligase and mainly facilitates protein degradation through ubiquitin-proteasome system [31]. As shown in Fig. 7A–B, *in vivo* and *in vitro* ubiquitination assays revealed that TRIM7 stimulated NCOA4 ubiquitination. K48 and K63 are classical ubiquitinated sites for E3 ubiquitin ligase, and TRIM7 has been reported to modulate protein K48- and K63-linked ubiquitination [29,31]. To identify the chain linkage of ubiquitinated NCOA4, we generated two ubiquitin mutants, K48R and K63R. As shown in Fig. 7C, TRIM7 facilitated efficient ubiquitination of NCOA4 using K63R ubiquitin; however, ubiquitination was significantly reduced when K48R-mutant ubiquitin was used. Thus, TRIM7 mainly promoted NCOA4 ubiquitination with K48-linked ubiquitin chains. To further determine whether TRIM7 altered NCOA4 protein stability, A172 cells with or without TRIM7 overexpression were treated with CHX to inhibit protein synthesis. As shown in Fig. 7D, TRIM7 overexpression dramatically slowed the degradation of NCOA4. And this degradation was mainly mediated through the ubiquitin-proteasome system (Fig. 7E). The RING finger of E3 ubiquitin ligases is essential for ubiquitination, and we generated a Flag-TRIM7 CA plasmid to destroy the integrity of the RING domain. As shown in Fig. 7F–G, this Flag-TRIM7 CA mutant plasmid failed to destabilize NCOA4 protein. In addition, we also generated a Flag-TRIM7 WA plasmid to block the interaction of the RING domain with ubiquitin-conjugating enzymes. As expected, NCOA4 protein stability was also unaffected by this Flag-TRIM7 WA plasmid (Fig. 7F–G). As

shown in Fig. 7H, we found that TRIM7 directly bound to NCOA4, and then, we generated different truncated TRIM7 plasmids to determine the potential interaction domains. Intriguingly, the Flag-TRIM7△PS mutant plasmid failed to interact with NCOA4, indicating the necessity of its C-terminal PRY/SPRY domain in TRIM7-NCOA4 interaction (Fig. 7H). Thus, these data imply that TRIM7 directly binds to and ubiquitinates NCOA4 using K48-linked chains.

3.8. TRIM7 deletion sensitizes human glioblastoma cells to TMZ therapy

TMZ-based chemotherapy is identified as a first-line treatment for human glioblastoma; therefore, we evaluated whether TRIM7-KO A172 cells were more sensitive to TMZ treatment *in vitro* and *in vivo*. As shown in Fig. 8A, TRIM7-KO A172 cells exhibited lower viability upon TMZ stimulation, compared to WT A172 cells. Meanwhile, TMZ-induced proliferation inhibition was more severe in TRIM7-KO A172 cells (Fig. 8B). Additionally, TRIM7 ablation further promoted glioblastoma cell death in the presence of TMZ, as evidenced by the increased LDH releases (Fig. 8C). In line with the *in vitro* findings, TRIM7-KO A172 cells also presented smaller tumor size *in vivo* upon TMZ treatment (Fig. 8D–E). Besides, we also verified the role of TRIM7 in human GSCs and PDX models. As shown in Fig. 8F–H, TRIM7 silence further inhibited survival and induced death of human GSCs. And TRIM7 silence also suppressed the growth of human glioblastoma in PDX models, as evidenced by the decreased tumor volume and weight (Fig. 8I–J). Overall, our findings demonstrate that TRIM7 deletion sensitizes human glioblastoma cells to TMZ therapy.

4. Discussion

Glioblastoma is one of the primary causes of cancer-related deaths in adults, and the majority of glioblastoma patients dies within 2 years despite the tremendous efforts in recent years. Gene-based target therapy is identified as a promising therapeutic strategy to treat various human cancers, including the glioblastoma. Herein, TRIM7 expression was found to be increased in human glioblastoma cells and tissues. TRIM7 silence induced, while TRIM7 overexpression suppressed intracellular iron accumulation, lipid peroxidation and ferroptotic cell death of human glioblastoma cells. Mechanistically, we demonstrated that TRIM7 directly bound to and ubiquitinated NCOA4 using K48-linked chains and subsequently reduced NCOA4 expression, thereby inhibiting the degradation of ferritin and decreasing intracellular iron levels

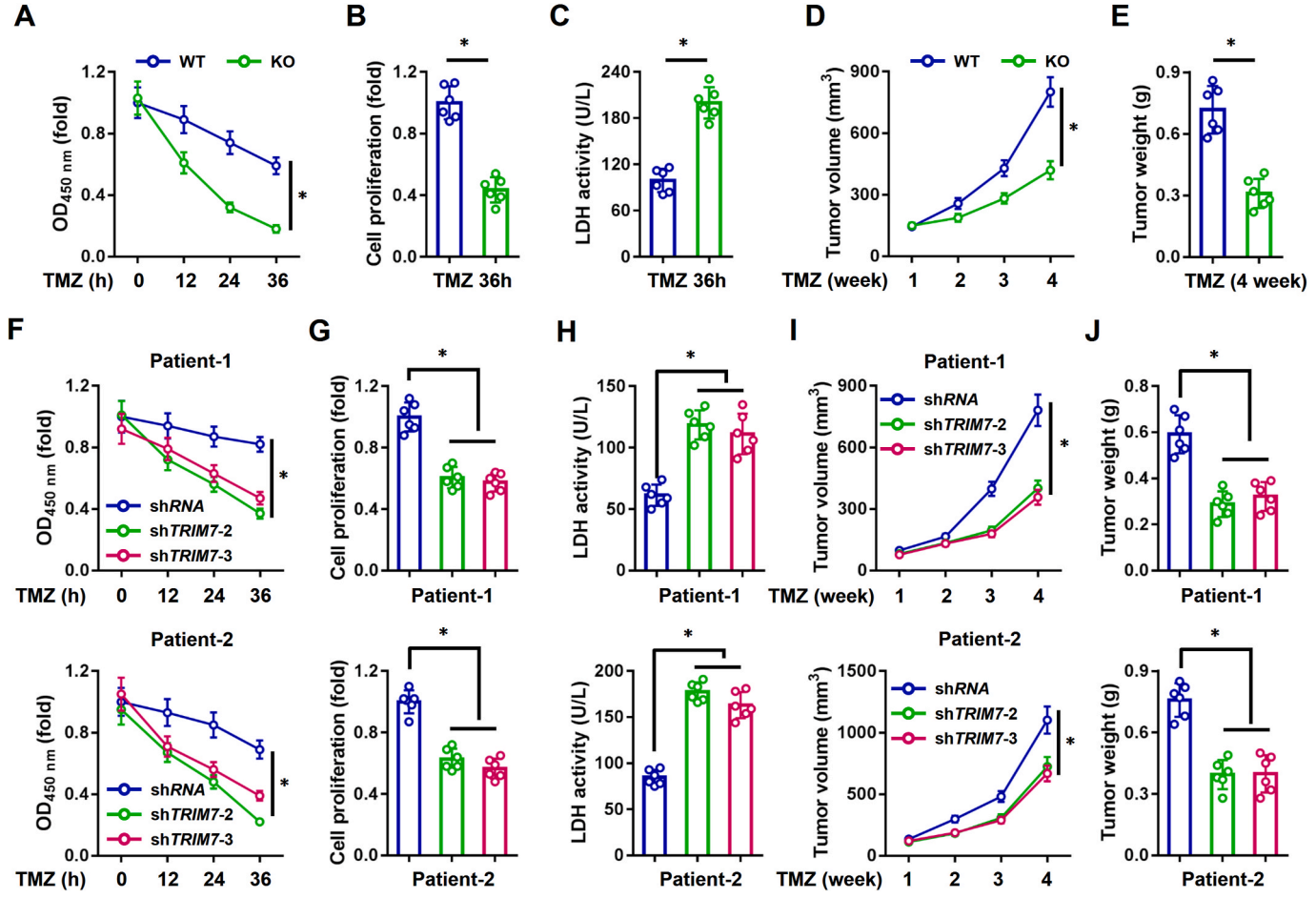

Fig. 8. TRIM7 deletion sensitizes human glioblastoma cells to TMZ therapy. (A) TRIM7-KO or WT A172 cells were treated with TMZ, and cell viability was detected using CCK-8 assay at indicating times. (B) Cell proliferation was assessed by BrdU assay at 36 h. (C) LDH releases from human glioblastoma cells to the medium at 36 h. (D) Tumor volume over time from mice inoculated with TRIM7-KO or WT A172 cells in the presence of TMZ treatment. (E) Tumor weight at 4 weeks from mice inoculated with TRIM7-KO or WT A172 cells in the presence of TMZ treatment. (F) Stable TRIM7-deficient or control GSCs were cultured and exposed to CCK-8 assay to evaluate cell viability. (G) Cell proliferation was assessed by BrdU assay at 72 h. (H) LDH releases from human GSCs to the medium at 72 h. (I) Tumor volume over time in PDX models with TMZ treatment. (J) Tumor weight at 4 weeks in PDX models with TMZ treatment. $N = 6$ for each group. All values are presented as the mean ± S.D., $^*P < 0.05$ is considered statistically significant.

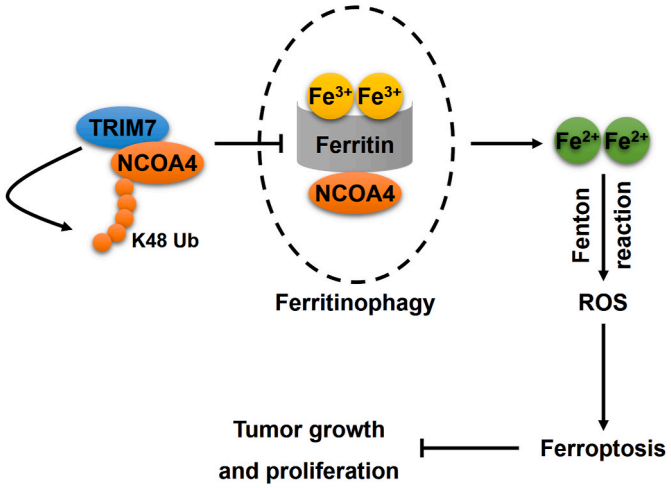

Fig. 9. A proposed molecular model of TRIM7 in regulating ferroptosis of human glioblastoma cells. TRIM7 directly binds to and ubiquitinates NCOA4 using K48-linked chains and subsequently reduces NCOA4 expression, thereby inhibiting the degradation of ferritin and decreasing intracellular iron levels, which then prevents lipid peroxidation and ferroptotic cell death of human glioblastoma cells.

(Fig. 9). More importantly, TRIM7 deficiency could sensitize human glioblastoma cells to TMZ treatment. These data reveal that TRIM7 is implicated in the regulation of intracellular iron metabolism and ferroptosis, and it is a promising therapeutic candidate to treat human glioblastoma.

Intracellular iron is essential for the growth and proliferation of various tumor cells, but it can also induce toxic lipid-based ROS generation through the Fenton reaction and facilitates ferroptotic cell death. Changes in iron homeostasis are identified as a key metabolic hallmark of human cancer, and iron metabolic reprogramming and dysfunction have also been shown to occur in human glioblastoma [19,56]. TF is an important iron-transport protein and mediates majority of the cellular iron uptake through binding to the cell-surface TFR, and then the TF/TFR complex is internalized by receptor-mediated endocytosis and releases iron into the cytosol [57]. However, in the present study, neither TF nor TFR expression was affected by TRIM7 silence in human glioblastoma cells. FPN1, the only discovered iron export protein in mammals, plays critical roles in pumping out intracellular iron. Accordingly, a very recent study by Tang et al. has demonstrated downregulating FPN1 induced significant increases of intracellular ferrous iron levels, lipid peroxidation and ferroptosis of human lung cancer cells [12]. It is well-accepted that intracellular iron is mainly stored by ferritin, and that ferritin downregulation facilitates the releases of free iron [58]. In addition, previous findings by Brown et al. indicated that ferritin could also transport iron out of the cell through the formation of ferritin-containing multivesicular bodies and exosomes [59]. Therefore, the ferritin protein level is essential for intracellular iron homeostasis. Autophagy performs housekeeping roles through controlling the degradation and recycling of some cytoplasmic proteins [60–62]. Ferritinophagy is a kind of selective autophagy responsible for the degradation of intracellular ferritin, which is mainly mediated by the cargo receptor, NCOA4 [16,63,64]. Using quantitative proteomics, Mancias et al. found that NCOA4 was highly enriched in autophagosomes, and that both FTH1 and ferritin light polypeptide 1 served as the substrates for NCOA4-mediated ferritinophagy [16]. As expected, emerging studies have demonstrated an indispensable role of NCOA4-associated ferritinophagy in intracellular iron homeostasis and cell ferroptosis in different cell types, including human glioblastoma cells. Zhang et al. recently reported that NCOA4 elevation led to degradation of ferritin and releases of ferrous iron, and that NCOA4 silence significantly decreased ferrous iron levels and ferroptosis in human glioblastoma cells [17]. Herein, we found that NCOA4 expression was upregulated, while FTH1 expression was downregulated in TRIM7-silenced human glioblastoma cells. And NCOA4 knockdown or autophagic inhibitors could significantly suppress TRIM7 silence-induced cell ferroptosis. In addition, iron chelators also inhibited ferroptosis in human glioblastoma cells by TRIM7 deficiency, indicating the central role of iron dysfunction in TRIM7-regulated ferroptosis.

Ubiquitination is an important post-translational modification of proteins and participates in a broad range of biological processes through promoting protein degradation. Protein ubiquitination mainly involves an E1 ubiquitin-activating enzyme, an E2 ubiquitin-conjugating enzyme and a substrate-specific E3 ubiquitin ligase [65–67]. TRIMs are a family of E3 ubiquitin ligases and stimulate protein degradation through ubiquitin-proteasome system [68,69]. TRIM7 is a member of TRIMs family and functions as an E3 ubiquitin ligase because of the presence of a RING domain [28]. Herein, we also found that the RING finger in TRIM7 was required for its ubiquitination of NCOA4, and that destroying the integrity of its RING domain blocked TRIM7-mediated degradation of NCOA4. In addition, we observed that TRIM7 directly bound to NCOA4 through its C-terminal PRY/SPRY domain.

In summary, we for the first time demonstrate that TRIM7 modulates NCOA4-mediated ferritinophagy and ferroptosis in glioblastoma cells, and our findings provide a novel insight into the progression and treatment for human glioblastoma.

Author contributions

KQL, BYC, ABX, YFZ, FHG and ZW conceived the study hypothesis. KQL, BYC, ABX, JLS, KXL, KH and RRH performed the experiments. KQL, BYC, WY and WLJ analyzed the data. KQL, BYC, YFZ and FHG wrote the first draft of the paper. KQL, FHG and ZW edited the paper and supervised all the work. All authors reviewed the results, made revisions as needed and approved the final version of the manuscript.

Funding

This work was supported by grants from the Key projects jointly constructed by the Ministry and the province of Zhejiang Medical and Health Science and Technology Project (WKJ-ZJ-2019) and Zhejiang Medical and Health Science and Technology Project (2022KY529) and the National Natural Science Foundation of China (82100368).

Declaration of competing interest

The authors report no potential conflicts of interest in this work.

Appendix A. Supplementary data

Supplementary data to this article can be found online at https://doi.org/10.1016/j.redox.2022.102451.

References

[1] R. Stupp, W.P. Mason, M.J. van den Bent, et al., Radiotherapy plus concomitant and adjuvant temozolomide for glioblastoma, N. Engl. J. Med. 352 (10) (2005) 987–996.
[2] W.Y. Bae, J.S. Choi, S. Nam, J.W. Jeong, beta-arrestin 2 stimulates degradation of HIF-1alpha and modulates tumor progression of glioblastoma, Cell Death Differ. 28 (11) (2021) 3092–3104.
[3] F. Li, S. Chen, J. Yu, et al., Interplay of m(6) A and histone modifications contributes to temozolomide resistance in glioblastoma, Clin. Transl. Med. 11 (9) (2021) e553.
[4] X. Zheng, W. Li, H. Xu, et al., Sinomenine ester derivative inhibits glioblastoma by inducing mitochondria-dependent apoptosis and autophagy by PI3K/AKT/mTOR and AMPK/mTOR pathway, Acta Pharm. Sin. B 11 (11) (2021) 3465–3480.
[5] C.M. Cushing, M.S. Petronek, K.L. Bodeker, et al., Magnetic resonance imaging (MRI) of pharmacological ascorbate-induced iron redox state as a biomarker in subjects undergoing radio-chemotherapy, Redox Biol. 38 (2021), 101804.

[6] X. Chen, R. Kang, G. Kroemer, D. Tang, Organelle-specific regulation of ferroptosis, Cell Death Differ. 28 (10) (2021) 2843–2856.
[7] M. Shen, Y. Li, Y. Wang, et al., N(6)-methyladenosine modification regulates ferroptosis through autophagy signaling pathway in hepatic stellate cells, Redox Biol. 47 (2021), 102151.
[8] Y. Liu, Z. Song, Y. Liu, et al., Identification of ferroptosis as a novel mechanism for antitumor activity of natural product derivative a2 in gastric cancer, Acta Pharm. Sin. B 11 (6) (2021) 1513–1525.
[9] J. Wang, X. Yin, W. He, W. Xue, J. Zhang, Y. Huang, SUV39H1 deficiency suppresses clear cell renal cell carcinoma growth by inducing ferroptosis, Acta Pharm. Sin. B 11 (2) (2021) 406–419.
[10] W.D. Bao, P. Pang, X.T. Zhou, et al., Loss of ferroportin induces memory impairment by promoting ferroptosis in Alzheimer's disease, Cell Death Differ. 28 (5) (2021) 1548–1562.
[11] Y. Liu, B.A. Bell, Y. Song, et al., Intraocular iron injection induces oxidative stress followed by elements of geographic atrophy and sympathetic ophthalmia, Aging Cell 20 (11) (2021), e13490.
[12] Z. Tang, W. Jiang, M. Mao, J. Zhao, J. Chen, N. Cheng, Deubiquitinase USP35 modulates ferroptosis in lung cancer via targeting ferroportin, Clin. Transl. Med. 11 (4) (2021), e390.
[13] N. Kong, X. Chen, J. Feng, et al., Baicalin induces ferroptosis in bladder cancer cells by downregulating FTH1, Acta Pharm. Sin. B 11 (12) (2021) 4045–4054.
[14] F. Ito, K. Kato, I. Yanatori, T. Murohara, S. Toyokuni, Ferroptosis-dependent extracellular vesicles from macrophage contribute to asbestos-induced mesothelial carcinogenesis through loading ferritin, Redox Biol. 47 (2021), 102174.
[15] P. Wang, Y. Cui, Q. Ren, et al., Mitochondrial ferritin attenuates cerebral ischaemia/reperfusion injury by inhibiting ferroptosis, Cell Death Dis. 12 (5) (2021) 447.
[16] J.D. Mancias, X. Wang, S.P. Gygi, J.W. Harper, A.C. Kimmelman, Quantitative proteomics identifies NCOA4 as the cargo receptor mediating ferritinophagy, Nature 509 (7498) (2014) 105–109.
[17] Y. Zhang, Y. Kong, Y. Ma, et al., Loss of COPZ1 induces NCOA4 mediated autophagy and ferroptosis in glioblastoma cell lines, Oncogene 40 (8) (2021) 1425–1439.
[18] T. Oliveira, E. Hermann, D. Lin, W. Chowanadisai, E. Hull, M. Montgomery, HDAC inhibition induces EMT and alterations in cellular iron homeostasis to augment ferroptosis sensitivity in SW13 cells, Redox Biol. 47 (2021), 102149.
[19] C. Legendre, E. Garcion, Iron metabolism: a double-edged sword in the resistance of glioblastoma to therapies, Trends Endocrinol. Metabol. 26 (6) (2015) 322–331.
[20] X. Zhu, Y. Zhou, Y. Ou, et al., Characterization of ferroptosis signature to evaluate the predict prognosis and immunotherapy in glioblastoma, Aging (Albany NY) 13 (13) (2021) 17655–17672.
[21] M. Buccarelli, M. Marconi, S. Pacioni, et al., Inhibition of autophagy increases susceptibility of glioblastoma stem cells to temozolomide by igniting ferroptosis, Cell Death Dis. 9 (8) (2018) 841.
[22] T.C. Chen, J.Y. Chuang, C.Y. Ko, et al., AR ubiquitination induced by the curcumin analog suppresses growth of temozolomide-resistant glioblastoma through disrupting GPX4-Mediated redox homeostasis, Redox Biol. 30 (2020), 101413.
[23] S. Zeng, Z. Zhao, S. Zheng, et al., The E3 ubiquitin ligase TRIM31 is involved in cerebral ischemic injury by promoting degradation of TIGAR, Redox Biol. 45 (2021), 102058.
[24] L.M. Humphreys, P. Smith, Z. Chen, S. Fouad, V. D'Angiolella, The role of E3 ubiquitin ligases in the development and progression of glioblastoma, Cell Death Differ. 28 (2) (2021) 522–537.
[25] Y. Liu, R. Raheja, N. Yeh, et al., TRIM3, a tumor suppressor linked to regulation of p21(Waf1/Cip1.), Oncogene 33 (3) (2014) 308–315.
[26] S. Feng, X. Cai, Y. Li, X. Jian, L. Zhang, B. Li, Tripartite motif-containing 14 (TRIM14) promotes epithelial-mesenchymal transition via ZEB2 in glioblastoma cells, J. Exp. Clin. Cancer Res. 38 (1) (2019) 57.
[27] J. Ji, K. Ding, T. Luo, et al., TRIM22 activates NF-kappaB signaling in glioblastoma by accelerating the degradation of IkappaBalpha, Cell Death Differ. 28 (1) (2021) 367–381.
[28] W. Fan, K.B. Mar, L. Sari, et al., TRIM7 inhibits enterovirus replication and promotes emergence of a viral variant with increased pathogenicity, Cell 184 (13) (2021) 3410–3425.
[29] A. Chakraborty, M.E. Diefenbacher, A. Mylona, O. Kassel, A. Behrens, The E3 ubiquitin ligase Trim7 mediates c-Jun/AP-1 activation by Ras signalling, Nat. Commun. 6 (2015) 6782.
[30] C. Zhou, Z. Zhang, X. Zhu, et al., N6-Methyladenosine modification of the TRIM7 positively regulates tumorigenesis and chemoresistance in osteosarcoma through ubiquitination of BRMS1, EBioMedicine 59 (2020), 102955.
[31] L. Zhu, C. Qin, T. Li, et al., The E3 ubiquitin ligase TRIM7 suppressed hepatocellular carcinoma progression by directly targeting Src protein, Cell Death Differ. 27 (6) (2020) 1819–1831.
[32] J. Jin, Z. Lu, X. Wang, et al., E3 ubiquitin ligase TRIM7 negatively regulates NF-kappa B signaling pathway by degrading p65 in lung cancer, Cell. Signal. 69 (2020), 109543.
[33] C. Yuan, J. Liu, L. Liu, et al., TRIM7 suppresses cell invasion and migration through inhibiting HIF-1alpha accumulation in clear cell renal cell carcinoma, Cell Biol. Int. 46 (4) (2022) 554–567.
[34] M. Luo, L. Wu, K. Zhang, et al., miR-137 regulates ferroptosis by targeting glutamine transporter SLC1A5 in melanoma, Cell Death Differ. 25 (8) (2018) 1457–1472.
[35] C. Hu, X. Zhang, M. Hu, et al., Fibronectin type III domain-containing 5 improves aging-related cardiac dysfunction in mice, Aging Cell 21 (3) (2022), e13556.
[36] X. Zhang, C. Hu, C.Y. Kong, et al., FNDC5 alleviates oxidative stress and cardiomyocyte apoptosis in doxorubicin-induced cardiotoxicity via activating AKT, Cell Death Differ. 27 (2) (2020) 540–555.
[37] C. Hu, X. Zhang, W. Wei, et al., Matrine attenuates oxidative stress and cardiomyocyte apoptosis in doxorubicin-induced cardiotoxicity via maintaining AMPKalpha/UCP2 pathway, Acta Pharm. Sin. B 9 (4) (2019) 690–701.
[38] X. Zhang, C. Hu, N. Zhang, et al., Matrine attenuates pathological cardiac fibrosis via RPS5/p38 in mice, Acta Pharmacol. Sin. 42 (4) (2021) 573–584.
[39] T. Gui, M. Liu, B. Yao, et al., TCF3 is epigenetically silenced by EZH2 and DNMT3B and functions as a tumor suppressor in endometrial cancer, Cell Death Differ. 28 (12) (2021) 3316–3328.
[40] J. Zhou, L. Wang, Q. Sun, et al., Hsa_circ_0001666 suppresses the progression of colorectal cancer through the miR-576-5p/PCDH10 axis, Clin. Transl. Med. 11 (11) (2021) e565.
[41] X. Zhang, C. Hu, X.P. Yuan, et al., Osteocrin, a novel myokine, prevents diabetic cardiomyopathy via restoring proteasomal activity, Cell Death Dis. 12 (7) (2021) 624.
[42] J. Koschel, G. Nishanth, S. Just, et al., OTUB1 prevents lethal hepatocyte necroptosis through stabilization of c-IAP1 during murine liver inflammation, Cell Death Differ. 28 (7) (2021) 2257–2275.
[43] Y. Hou, Q. Zhang, W. Pang, et al., YTHDC1-mediated augmentation of miR-30d in repressing pancreatic tumorigenesis via attenuation of RUNX1-induced transcriptional activation of Warburg effect, Cell Death Differ. 28 (11) (2021) 3105–3124.
[44] X. Zhang, C. Hu, Y.P. Yuan, et al., Endothelial ERG alleviates cardiac fibrosis via blocking endothelin-1-dependent paracrine mechanism, Cell Biol. Toxicol. 37 (6) (2021) 873–890.
[45] C. Hu, X. Zhang, P. Song, et al., Meteorin-like protein attenuates doxorubicin-induced cardiotoxicity via activating cAMP/PKA/SIRT1 pathway, Redox Biol. 37 (2020), 101747.
[46] W. Zhou, N. Kaneko, T. Nakagita, H. Takeda, J. Masumoto, A comprehensive interaction study provides a potential domain interaction network of human death domain superfamily proteins, Cell Death Differ. 28 (11) (2021) 2991–3008.
[47] E. Daveri, A.M. Adamo, E. Alfine, W. Zhu, P.I. Oteiza, Hexameric procyanidins inhibit colorectal cancer cell growth through both redox and non-redox regulation of the epidermal growth factor signaling pathway, Redox Biol. 38 (2021), 101830.
[48] C. Hu, X. Zhang, N. Zhang, et al., Osteocrin attenuates inflammation, oxidative stress, apoptosis, and cardiac dysfunction in doxorubicin-induced cardiotoxicity, Clin. Transl. Med. 10 (3) (2020) e124.
[49] X. Zhang, Z.G. Ma, Y.P. Yuan, et al., Rosmarinic acid attenuates cardiac fibrosis following long-term pressure overload via AMPKalpha/Smad3 signaling, Cell Death Dis. 9 (2) (2018) 102.
[50] L. Xu, L. Yin, Y. Qi, X. Tan, M. Gao, J. Peng, 3D disorganization and rearrangement of genome provide insights into pathogenesis of NAFLD by integrated Hi-C, Nanopore, and RNA sequencing, Acta Pharm. Sin. B 11 (10) (2021) 3150–3164.
[51] M.W. Park, H.W. Cha, J. Kim, et al., NOX4 promotes ferroptosis of astrocytes by oxidative stress-induced lipid peroxidation via the impairment of mitochondrial metabolism in Alzheimer's diseases, Redox Biol. 41 (2021), 101947.
[52] T.E. Miller, B.B. Liau, L.C. Wallace, et al., Transcription elongation factors represent in vivo cancer dependencies in glioblastoma, Nature 547 (7663) (2017) 355–359.
[53] H. Huang, S. Zhang, Y. Li, et al., Suppression of mitochondrial ROS by prohibitin drives glioblastoma progression and therapeutic resistance, Nat. Commun. 12 (1) (2021) 3720.
[54] X.N. Zhang, K.D. Yang, C. Chen, et al., Pericytes augment glioblastoma cell resistance to temozolomide through CCL5-CCR5 paracrine signaling, Cell Res. 31 (10) (2021) 1072–1087.
[55] Y. Ma, N. Tang, R.C. Thompson, et al., InsR/IGF1R pathway mediates resistance to EGFR inhibitors in glioblastoma, Clin. Cancer Res. 22 (7) (2016) 1767–1776.
[56] T. Basak, R.K. Kanwar, Iron imbalance in cancer: intersection of deficiency and overload, Cancer Med. (2022) undefined–undefined.
[57] Y. Wu, H. Jiao, Y. Yue, et al., Ubiquitin ligase E3 HUWE1/MULE targets transferrin receptor for degradation and suppresses ferroptosis in acute liver injury, Cell Death Differ. (2022) undefined–undefined.
[58] S. Kuno, H. Fujita, Y.K. Tanaka, Y. Ogra, K. Iwai, Iron-induced NCOA4 condensation regulates ferritin fate and iron homeostasis, EMBO Rep. (2022), e54278.
[59] C.W. Brown, J.J. Amante, P. Chhoy, et al., Prominin2 drives ferroptosis resistance by stimulating iron export, Dev. Cell 51 (5) (2019) 575–586.
[60] X. Chen, C. Yu, R. Kang, G. Kroemer, D. Tang, Cellular degradation systems in ferroptosis, Cell Death Differ. 28 (4) (2021) 1135–1148.
[61] H.Y. Tu, B.S. Yuan, X.O. Hou, et al., alpha-synuclein suppresses microglial autophagy and promotes neurodegeneration in a mouse model of Parkinson's disease, Aging Cell 20 (12) (2021), e13522.
[62] K. He, L. Nie, T. Ali, et al., Adiponectin alleviated Alzheimer-like pathologies via autophagy-lysosomal activation, Aging Cell 20 (12) (2021), e13514.
[63] K. Wang, Z. Zhang, H.I. Tsai, et al., Branched-chain amino acid aminotransferase 2 regulates ferroptotic cell death in cancer cells, Cell Death Differ. 28 (4) (2021) 1222–1236.
[64] N. Santana-Codina, A. Gikandi, J.D. Mancias, The role of NCOA4-mediated ferritinophagy in ferroptosis, Adv. Exp. Med. Biol. 1301 (2021) 41–57.
[65] Y. Rong, J. Fan, C. Ji, et al., USP11 regulates autophagy-dependent ferroptosis after spinal cord ischemia-reperfusion injury by deubiquitinating Beclin 1, Cell Death Differ. 29 (6) (2021) 1164–1175.

[66] Z.G. Wang, H.E. Xu, F.M. Cheng, et al., Donor BMSC-derived small extracellular vesicles relieve acute rejection post-renal allograft through transmitting Loc108349490 to dendritic cells, Aging Cell 20 (10) (2021), e13461.
[67] A. Tyagi, S. Haq, S. Ramakrishna, Redox regulation of DUBs and its therapeutic implications in cancer, Redox Biol. 48 (2021), 102194.
[68] D.B. Zou, Z. Mou, W. Wu, H. Liu, TRIM33 protects osteoblasts from oxidative stress-induced apoptosis in osteoporosis by inhibiting FOXO3a ubiquitylation and degradation, Aging Cell 20 (7) (2021), e13367.
[69] J. Zhao, B. Cai, Z. Shao, et al., TRIM26 positively regulates the inflammatory immune response through K11-linked ubiquitination of TAB1, Cell Death Differ. 28 (11) (2021) 3077–3091.